Submitted: 18 September, 2022 Accepted: 01 February, 2023 Published: 15 October, 2023 DOI:10.22514/ejgo.2023.074

ORIGINAL RESEARCH

European Journal of Gynaecological Oncology

iTRAQ-based proteomics analysis reveals novel candidates for platinum resistance of epithelial ovarian cancer

Yuanjing Wang[1,*], Yumei Wu[2]

[1]Department of Radiation Therapy Center, Beijing Obstetrics and Gynecology Hospital, Capital Medical University (Beijing Maternal and Child Health Care Hospital), 100006 Beijing, China
[2]Department of Gynecological Oncology, Beijing Obstetrics and Gynecology Hospital, Capital Medical University (Beijing Maternal and Child Health Care Hospital), 100006 Beijing, China

***Correspondence**
wangyuanjing@mail.ccmu.edu.cn
(Yuanjing Wang)

Abstract

Platinum-based chemotherapy is commonly used in the treatment of various cancers, including epithelial ovarian cancer (EOC). However, in EOC, chemotherapy failure is mainly caused by platinum resistance. In this present study, we aimed to identify novel biomarkers for predicting platinum chemosensitivity. Fresh specimens of 16 serous high-grade ovarian cancer (HGSC) cases were collected during cytoreductive surgery. Isobaric tags were used to identify differentially expressed proteins in platinum-resistant samples (n = 8) and platinum-sensitive samples (n = 8). Compared to platinum-sensitive samples, 741 significantly differentially expressed proteins were detected, of which 325 were upregulated and 416 were downregulated. To validate the isobaric tags for relative and absolute quantification (iTRAQ) method, western blotting was performed on two upregulated proteins, angiomotin-like protein 1 (AMOTL1) and Lumican. The results showed that platinum-resistant tumor samples expressed significantly higher levels of AMOTL1 and Lumican than platinum-sensitive tumor samples. Altogether, we identified candidate proteins related to platinum resistance in ovarian cancer. Both AMOTL1 and Lumican seem to be promising biomarkers that could distinguish between platinum-resistant and platinum-sensitive EOC.

Keywords

Epithelial ovarian cancer; Platinum resistance; Angiomotin-like protein 1; Lumican; Isobaric tags for relative and absolute quantitation

1. Introduction

Presently, ovarian cancer is the major cause of cancer-related deaths among all gynecological malignancies worldwide, accounting for about 225,000 new cases and 140,200 cancer-specific deaths annually [1]. The most commonly seen histological type of EOC is the high-grade serous ovarian cancer subtype (HGSC) [2]. Platinum-based chemotherapy and primary debulking surgery (PDS) are the current gold treatment standards for advanced EOC [3]. However, since the past decade, the mortality rate of EOC patients has remained unacceptably high, primarily due to the development of chemoresistance in those who initially responded well to platinum-based chemotherapy [4]. Even though targeted therapy has been intensively sought in EOC, the five-year survival rate for late-stage cases remains under 29% due to disease relapse and drug resistance [5]. Therefore, the identification of novel specific markers that can predict platinum chemosensitivity is highly necessary to improve EOC patients' treatment outcomes.

Retrospective studies on platinum-based chemotherapy have shown that recurrent EOC can be divided as platinum-sensitive or platinum-resistant based on the platinum-free interval (PFI). Cases with a PFI >6 months after the finalization of platinum-based therapy can be classified as "platinum-sensitive" ovarian cancer, while those with a PFI <6 months can be classified as "platinum-resistant" ovarian cancer [6]. Even though most platinum-sensitive cases can achieve a favorable therapeutic response to initial treatment, most will eventually become platinum-resistant. The molecular mechanisms underlying the development of platinum resistance are not yet fully understood and have negatively impacted the treatment outcomes of EOC patients [7]. Consequently, identifying biomarkers for platinum-resistant ovarian cancer would help patients and clinicians make better-informed treatment decisions.

In this current study, liquid chromatography-tandem mass spectrometry (LC-MS/MS) combined with iTRAQ analysis was performed to identify differentially expressed proteins in ovarian cancer samples among platinum-resistant and platinum-sensitive patients. iTRAQ analysis employs a gel-free proteomics mass spectrometry method that allows the identification and quantification of the relative abundance of peptides in a complex mixture. Given the differential pattern of two-dimensional gel electrophoresis for protein samples, LC-MS/MS can reveal additional biological information, such as isoelectric point drift or molecular weight variations,

according to the protein functions involved [8]. iTRAQ analysis coupled with LC-MS/MS is more sensitive and precise than conventional proteomics methods, particularly for detecting low-abundance proteins, making it a more capable tool for quantifying expressed proteins in biological samples [9]. In recent years, iTRAQ analysis has become widely used for identifying differentially expressed protein markers in ovarian cancer research. Several studies have used iTRAQ to discover novel biomarkers in EOC by analyzing cells, tissues, tumor fluids and serum samples [10].

In this present study, we aimed to identify potential biomarkers related to the mechanism of platinum resistance in ovarian cancer. Furthermore, we aimed to enhance our understanding of the mechanism underlying platinum resistance in ovarian cancer by identifying and validating novel drug targets associated with platinum resistance.

2. Materials and methods

2.1 Study cohorts and tumor samples

Sixteen HGSC cases were included for the iTRAQ-based proteomic analysis, and their baseline characteristics are shown in Table 1. Fresh specimens were collected during cytoreductive surgery following the initial diagnosis. In this cohort, platinum sensitivity and resistance (response to treatment) were considered as the study selection criteria, with neither age nor the International Federation of Gynecology and Obstetrics (FIGO) taken into consideration. In this study, platinum sensitivity referred to the absence of recurrence during half a year post-chemotherapy using first-line platinum agents. The validation cohort of the iTRAQ data was composed of all the patients from a previous prospective study (Table 2). Sixty fresh tumor tissue samples were obtained from EOC cases who underwent primary debulking procedures at the Beijing Shijitan Hospital from January 2013 to December 2015. Each fresh sample was collected from macroscopically visible tumors in the operating room, and two samples of approximately 0.5 cm were snap-frozen with liquid nitrogen and kept at −80 ℃ for subsequent tests. As part of the routine diagnostics, histopathology was conducted by two experienced pathologists at the Department of Pathology (Beijing Shijitan Hospital) to determine the tumor stage and degree of malignancy.

2.2 iTRAQ combined with LC-MS/MS

iTRAQ analyses were performed on resistant (n = 8, R group) and sensitive specimens (n = 8, S group) to identify proteins related to platinum resistance. Homogenization and sonication of frozen tumor samples (180 W) were performed using a cell disperser and 0.5% sodium dodecyl sulfate (SDS). Centrifugation was conducted at 2000 g for half an hour at four centigrade degrees to remove cell debris. Once the supernatant had been collected, the protein concentration was determined using the Bradford assay. Then, the protein (100 μg per condition) was treated with 55 mM iodoacetamide and 10 mM dithiothreitol for reduction and alkylation. Next, trypsin (Promega Corporation, Madison, WI, USA) was used to digest the proteins, and iTRAQ reagents (Thermo Fisher Scientific, Inc., Waltham, MA, USA; Applied Biosystems) were used

TABLE 1. Baseline characteristics of cases in the iTRAQ-based proteomic analysis cohort (n = 16).

Characteristics	Platinum-sensitive, n (%)	Platinum-resistant, n (%)
Total cases	8	8
Histology		
Serous	8 (100%)	8 (100%)
Grade 3†	8 (100%)	8 (100%)
FIGO* classification		
Stage I	2	0
Stage II	0	1
Stage III	6	7

**FIGO = the International Federation of Gynecology and Obstetrics. †Grade 3 = high grade tumors.*

TABLE 2. Baseline characteristics of the validation cohort (n = 60).

Characteristics	n	(%)
All	60	
Histology		
Serous	46	76.7
Mucinous	2	3.3
Clear cell	6	10.0
Endometrioid	4	6.7
Transitional cell	2	3.3
FIGO* classification		
Stage I	9	15.0
Stage II	7	11.7
Stage III	44	73.3
Grade†		
Grade 2/1	12	20.0
Grade 3	48	80.0
Response to platinum therapy‡		
Sensitive	35	58.3
Resistant	25	41.6
Tumor type		
Primary	54	90.0
Recurrent	6	10.0

**FIGO = the International Federation of Gynecology and Obstetrics. ‡Sensitive: recurrence 6 months post first-line treatment using platinum agents; Resistant: recurrence within the first 6 months since starting first-line treatment using platinum agents.†Grade-Grade 2/1 indicates low-grade tumors, and Grade 3 indicates high-grade tumors.*

TABLE 3. The 50 most upregulated and 50 most down-regulated proteins in platinum-resistant EOC samples compared to the control.

Gene Name	Gene symbol	Protein description	Fold change for S/R
Upregulated in R samples			
Q03692	COL10A1	Collagen alpha-1 (X) chain	0.317
Q8IY63	AMOTL1	Angiomotin-like protein 1	0.330
P15090	FABP4	Adipocyte fatty acid-binding protein	0.356
P02768	ALB	Serum amyloid A protein	0.393
Q9UPU7	TBC1D2B	TBC1 domain family member 2B	0.413
P51884	LUM	Lumican	0.419
P51888	PRELP	Prolargin	0.424
P10451	SPP1	Osteopontin	0.425
P10909	CLU	Clusterin	0.435
P05156	CFI	Complement factor I	0.457
P13647	KRT5	Keratin, type II cytoskeletal 5	0.470
P04196	HRG	Histidine-rich glycoprotein	0.471
Q8NG11	TSPAN14	Tetraspanin-14	0.482
O75882	ATRN	Attractin	0.502
Q8WUP2	FBLIM1	Filamin-binding LIM protein 1	0.503
P49747	COMP	Cartilage oligomeric matrix protein	0.510
P68871	HBB	Hemoglobin subunit beta	0.512
P00325	ADH1B	Alcohol dehydrogenase 1B	0.514
Q969E4	TCEAL3	Transcription elongation factor A protein-like 3	0.518
P00738	HP	Haptoglobin	0.518
P07602	PSAP	Proactivator polypeptide	0.523
P25311	AZGP1	Zinc-alpha-2-glycoprotein	0.529
Q6NYC8	PPP1R18	Phostensin	0.533
P07951	TPM2	Tropomyosin beta chain	0.538
P02763	ORM1	Alpha-1-acid glycoprotein 1	0.544
P02765	AHSG	Alpha-2-HS-glycoprotein	0.544
P01009	SERPINA1	Alpha-1-antitrypsin	0.548
P84157	MXRA7	Matrix-remodeling-associated protein 7	0.552
P08294	SOD3	Extracellular superoxide dismutase [Cu-Zn]	0.551
P27658	COL8A1	Collagen alpha-1 (VIII) chain	0.553
Q03591	CFHR1	Complement factor H-related protein 1	0.564
P02790	HPX	Hemopexin	0.567
Q9HCY8	S100A14	Protein S100-A14	0.570
P07996	THBS1	Thrombospondin-1	0.573
P69905	HBA1	Hemoglobin subunit alpha	0.577
P36955	SERPINF1	Pigment epithelium-derived factor	0.578
P00751	CFB	Complement factor B	0.579
P04217	A1BG	Alpha-1B-glycoprotein	0.579
P22570	FDXR	NADPH: adrenodoxin oxidoreductase, mitochondrial	0.580
P02743	APCS	Serum amyloid P-component	0.581

TABLE 3. Continued.

Gene Name	Gene symbol	Protein description	Fold change for S/R
Q6NZI2	PTRF	Polymerase I and transcript release factor	0.582
P05452	CLEC3B	Tetranectin	0.582
P02774	GC	Vitamin D-binding protein	0.586
P02647	APOA1	Apolipoprotein A-I	0.586
P02768	ALB	Serum albumin	0.587
Q06828	FMOD	Fibromodulin	0.589
P06703	S100A6	Protein S100-A6	0.591
P21589	NT5E	5′-nucleotidase	0.591
P13611	VCAN	Versican core protein	0.593
Q01995	TAGLN	Transgelin	0.594
Downregulated in R samples			
Q9Y263	PLAA	Phospholipase A-2-activating protein	2.906
Q8NC56	LEMD2	LEM domain-containing protein 2	2.895
Q9H6Y7	RNF167	E3 ubiquitin-protein ligase RNF167	2.685
Q5TEJ8	THEMIS2	Protein THEMIS2	2.445
P23219	PTGS1	Prostaglandin G/H synthase 1	2.322
P67809	YBX1	Nuclease-sensitive element-binding protein 1	2.229
O60832	DKC1	H/ACA ribonucleoprotein complex subunit 4	2.202
P15328	FOLR1	Folate receptor alpha	2.082
O75688	PPM1B	Protein phosphatase 1B	1.932
Q86SX6	GLRX5	Glutaredoxin-related protein 5	1.921
Q14978	NOLC1	Nucleolar and coiled-body phosphoprotein 1	1.920
P06454	PTMA	Prothymosin alpha	1.899
P23297	S100A1	Protein S100-A1	1.879
O15231	ZNF185	Zinc finger protein 185	1.847
P32455	GBP1	Interferon-induced guanylate-binding protein 1	1.824
Q9UBN7	HDAC6	Histone deacetylase 6	1.822
Q63HN8	RNF213	RING finger protein 213	1.822
P04439	HLA-A	HLA class I histocompatibility antigen, A-3 alpha chain	1.821
P42224	STAT1	Signal transducer and activator of transcription 1-alpha/beta	1.752
P20591	MX1	Interferon-induced GTP-binding protein Mx1	1.794
P05161	ISG15	Interferon-induced 17 kDa protein	1.745
O14879	IFIT3	Interferon-induced protein with tetratricopeptide repeats 3	1.738
Q9Y2Q3	GSTK1	Glutathione S-transferase kappa 1	1.72
P10155	TROVE2	60 kDa SS-A/Ro ribonucleoprotein	1.696
P68431	HIST1H3A	Histone H3.1	1.694
Q9UL46	PSME2	Proteasome activator complex subunit 2	1.671
P06899	HIST1H2BJ	Histone H2B type 1-J	1.666
P46783	RPS10	40S ribosomal protein S10	1.654
P24539	ATP5F1	ATP synthase subunit b, mitochondrial	1.642
Q9Y2W1	THRAP3	Thyroid hormone receptor-associated protein 3	1.615
P53999	SUB1	Activated RNA polymerase II transcriptional co-activator p15	1.614
P62851	RPS25	40S ribosomal protein S25	1.610

TABLE 3. Continued.

Gene Name	Gene symbol	Protein description	Fold change for S/R
Q16610	ECM1	Extracellular matrix protein 1	1.594
P54709	ATP1B3	Sodium/potassium-transporting ATPase subunit beta-3	1.583
O76070	SNCG	Gamma-synuclein	1.569
Q9H1E3	NUCKS1	Nuclear ubiquitous casein and cyclin-dependent kinases substrate	1.560
P60866	RPS20	40S ribosomal protein S20	1.550
O43676	NDUFB3	NADH dehydrogenase (ubiquinone) 1 beta subcomplex subunit 3	1.548
P05141	SLC25A5	ADP/ATP translocase 2	1.537
Q06323	PSME1	Proteasome activator complex subunit 1	1.530
P26583	HMGB2	High mobility group protein B2	1.519
Q07021	C1QBP	Complement component 1 Q subcomponent-binding protein, mitochondrial	1.510
O60814	HIST1H2BK	Histone H2B type 1-K	1.499
P36542	ATP5C1	ATP synthase subunit gamma, mitochondrial	1.496
P09429	HMGB1	High mobility group protein B1	1.496
Q9Y446	PKP3	Plakophilin-3	1.494
P16401	HIST1H1B	Histone H1.5	1.491
P28838	LAP3	Cytosol aminopeptidase	1.490
Q03519	TAP2	Antigen peptide transporter 2	1.490
Q9NZ01	TECR	Trans-2,3-enoyl-CoA reductase	1.489

Abbreviations: S: platinum-sensitive samples; R: platinum-resistant samples.

to label the peptide mixtures following the manufacturer's instructions. S and R groups were tagged with iTRAQ 115 and 116, respectively. For strong cation exchange (SCX) chromatography, the labeled peptides were pooled and fractionated for 90 minutes at a flow rate of one millimeter per minute on a C-18 column (Phenomenex, Torrance, CA, USA; 100 A, 5 μm) using a linear gradient (0% to 100%) (solution B: 25% acetonitrile, 2 M potassium chloride (KCl), 10 mM potassium dihydrogen phosphate (KH_2PO_4), pH 3.0; solution A: 25% acetonitrile, 10 mM KH_2PO_4, pH 3.0). The obtained fractions were recombined into 16 fractions based on the chromatography results. After they were freeze-dried, the fractions (SCX column) were redissolved into an aqueous solution containing formic acid (0.1%), desalted using a strata-X C18 reversed-phase (RP) column (provided by Phenomenex), and as previously described [9], data-dependent nano-LC-MS/MS experiments were performed using quadrupole-Orbitrap mass spectrometry (Thermo Fisher, Scientific, Inc.; Q-Exactive) with a nano ultimate high-performance liquid chromatography (HPLC) (Phenomenex), following which the samples were extracted and analyzed.

2.3 Western blotting

Proteins (AMOTL1 and Lumican) were selected as putative differentially expressed proteins according to their corresponding fold change and high significance. The expression of AMOTL1 and Lumican was validated in EOC samples with varying chemosensitivities (S group, n = 35; R group, n = 25). After thawing, the tumor samples were rinsed twice with cold phosphate buffered saline (PBS) before lysis with a lysis buffer (10% glycerol, 1% Triton-x-100, 1 mM ethylenediaminetetraacetic acid (EDTA), 50 mM sodium fluoride (NaF), 50 mM tris (hydroxymethyl) aminomethane hydrochloride (Tris-HCl) pH 7.5, 150 mM sodium chloride (NaCl)) containing protease and phosphatase inhibitor cocktails (Bimake, Houston, TX, USA). In the first step, the lysates were blended with 4× Laemmli loading buffer and electrophoresed on an sodium dodecyl-sulfate polyacrylamide gel electrophoresis (SDS-PAGE) gel. After blocking with 5% non-fat milk (5%) in Tris-buffered saline containing Tween-20 (0.1%) for one hour at four degrees centigrade overnight, primary antibodies were applied to nitrocellulose membranes. The two primary antibodies were: rabbit anti-human polyclonal AMOTL1 (1:5000; Abcam, Cambridge, MA, USA, ab171976) and rabbit anti-human polyclonal Lumican (1:5000; Abcam, Cambridge, MA, USA, ab168348). After washing thrice with Tris-buffered saline (containing Tween-20), the membranes were incubated for 1–2 hours with a secondary antibody (goat anti-rabbit IgG, 1:5000; Abcam, Cambridge, MA, USA, ab97051) at room temperature. Then, an imaging system (two-color infrared; Li-COR Biosciences, Lincoln, NE, USA; Odyssey) was used to analyze the results. Protein quantification was normalized

to glyceraldehyde-3-phosphate dehydrogenase (GAPDH) (1:5000; Abcam, Cambridge, MA, USA, ab9485) expression level for each sample.

3. Data analysis

3.1 iTRAQ assay

Proteome Discoverer (version 1.3, Thermo Fisher Scientific, Waltham, MA, USA) and Mascot (version 2.3.0, Matrix Science, London, UK) were used to identify iTRAQ-labeled peptides and their corresponding proteins. In quantitative iTRAQ analysis, Protein Discoverer used the Pro GroupTM algorithm to select the peptides and calculate the reporter peak area, *p*-value and error factor. *p*-values were obtained by the empirical Bayes moderated *t*-test. In Mascot, Swiss-Prot human was chosen as the database, and trypsin was chosen as the digestion enzyme. The mass tolerance for fragment ions and parent ions was 0.05 Da and 0.02 Da, respectively. Cysteine carbamidomethylation and four-plex iTRAQ labeling were put in place, and two miscleavage sites (the maximum) might have occurred. Protein assembly involved the assignment of some shared peptides to groups of proteins (not a specific protein). Based on these shared peptides, the proteins were clustered together as a protein group. According to a false discovery rate (FDR) of $\leq$1%, all reported data were based on a 95% confidence level for protein identification. The sensitive control groups were normalized and used as a reference, resulting in all proteins from the sensitive control groups having a value of 1. During all runs of the experiment, acquired intensities were universally normalized. When the peak intensity of the reporter ion was $<$1% of the highest peak intensity, it was removed due to undependable quantification. In the current analysis, peptides (sensitive/resistant samples) quantified with a $\leq$0.83 old decrease and a $\geq$1.2 fold increase in concentration were considered upregulated and down-regulated in resistant samples, respectively. Based on Gene Ontology (GO) enrichment analysis, the Function Enrichment tool (FunRich; version 3.1.3; http://www.funrich.org) was used to classify the functions of the differentially expressed proteins. GO enrichment analysis was performed to determine related biological processes, molecular functions and biological pathways [11]. Statistically significant difference was considered for a log-rank value $p < 0.05$.

3.2 Statistical analysis

The Western blotting data were analyzed using unpaired Student's *t*-test and Mann-Whitney U test, where appropriate. The mean $\pm$ standard deviation was expressed for all results. Statistical analysis was conducted using GraphPad Prism 8 (GraphPad Software Inc., La Jolla, CA, USA). A *p*-value $<$ 0.05 was considered for determining statistical significance.

4. Results

4.1 iTRAQ analysis of HGSC patient samples

LC-MS/MS and iTRAQ analysis were performed on isolated peptides from freshly frozen tumor samples to identify differentially expressed proteins among platinum-sensitive and platinum-resistant ovarian cancer samples. According to the present study, 741 proteins were significantly differentially expressed among platinum-sensitive and platinum-resistant samples. The iTRAQ ratio's threshold (sensitive/resistant) in the resistant samples was $\geq$1.2 or $\leq$0.83, indicating a lower or higher protein expression level than in sensitive samples. Compared to platinum-sensitive samples, the platinum-resistant samples showed an upregulation in 325 proteins and a downregulation in 416 proteins. A summary of the 50 most upregulated and downregulated proteins is shown in Table 3.

4.2 Functional enrichment analysis

The possible biological processes, molecular functions and pathways of the differentially expressed proteins were investigated using the FunRich software. The top 6 enriched GO projects are shown in Fig. 1. The biological processes analyzed showed significant enrichment in proteins involved in cell growth and/or maintenance, protein metabolism, energy pathways, immune response and metabolism (Fig. 1A). For the analysis of molecular functions, the differentially expressed proteins comprised of "extracellular matrix structural constituent" and "transporter activity" (Fig. 1B). The biological pathways primarily comprised "epithelial-to-mesenchymal transition", "RNA polymerase I promoter clearance", and "GTP hydrolysis and joining of the 60 S ribosomal subunit" (Fig. 1C).

4.3 Validation by Western blotting

We validated two upregulated expressed proteins (AMOTL1 and Lumican) from the iTRAQ analysis in 60 ovarian cancer cases (Table 2). High fold changes (FC) and significant differences (AMOTL1, FC = 3.03, $p < 0.05$; Lumican, FC = 2.387, $p < 0.05$) were considered when selecting candidate proteins. The proteins were obtained from individuals with each sample type probed using commercially available antibodies. AMOTL1 and Lumican showed significantly different expressions in platinum-resistant groups compared to platinum-sensitive groups, which was concordant with the results of the iTRAQ. Platinum-resistant tumor samples expressed significantly higher levels of AMOTL1 and Lumican than platinum-sensitive tumor samples (p = 0.0005 and 0.01, respectively) (Fig. 2).

5. Discussion

Ovarian cancer is the most lethal type of gynecologic cancer in women [12]. Although platinum is the mainstay of systemic treatment for late-stage EOC, the emergence of platinum resistance remains a major challenge for most patients and clinicians. Given the poor prognosis associated with platinum-resistant ovarian cancer, there is an urgent need for improved therapeutic interventions and the identification of potential biomarkers. In this present study, we used the quantitative proteomic technique of iTRAQ to analyze proteins from platinum-resistant and platinum-sensitive tumor samples. Based on our analysis of individual protein expression levels, we identified 741 significantly differentially ex-

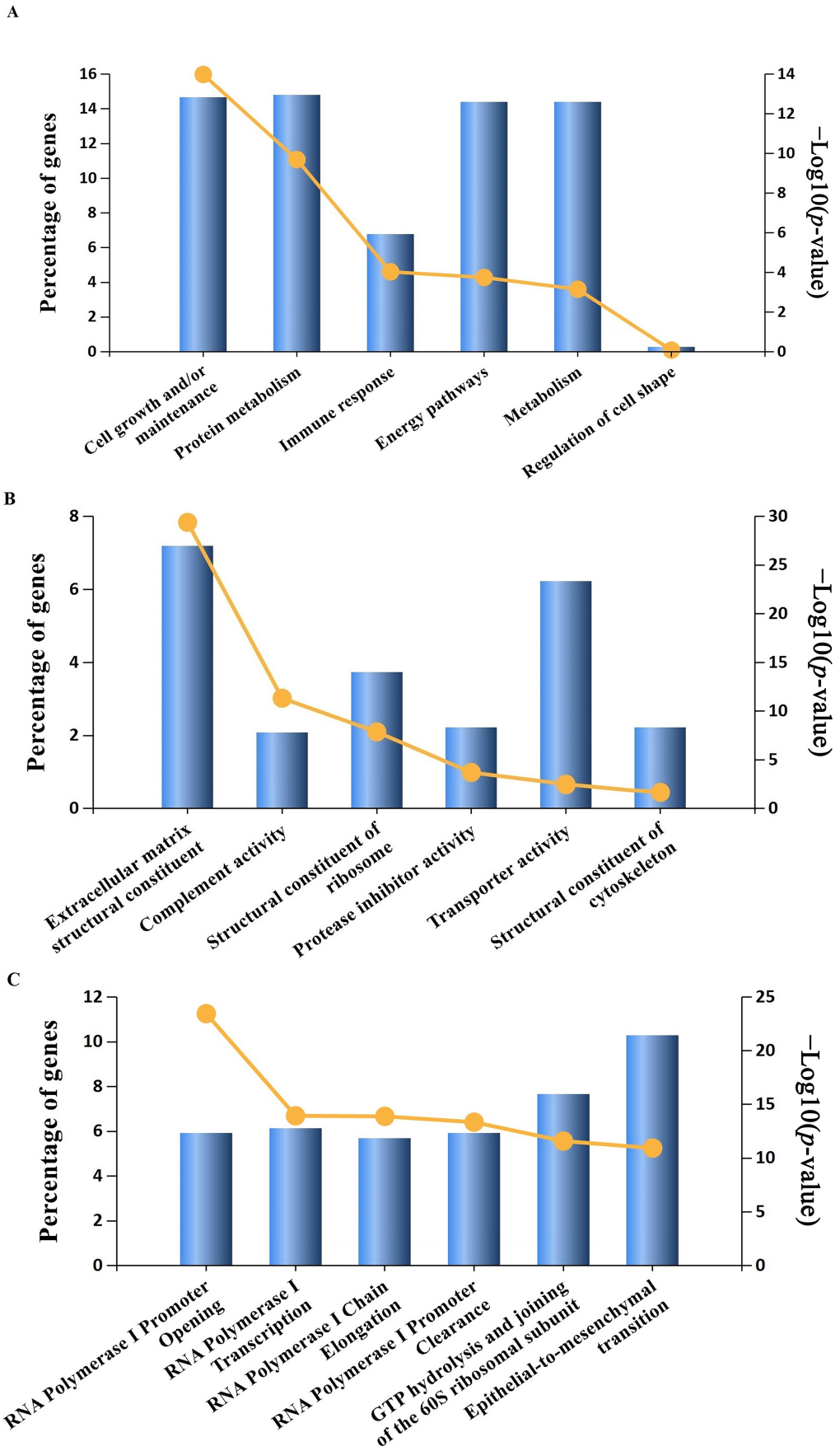

FIGURE 1. Analysis of differentially expressed proteins based on functional annotation and pathway enrichment. (A) Biological processes enrichment; (B) Molecular functions enrichment; (C) Biological pathways enrichment. The X-axis indicates detailed appellations of functional annotation and pathway enrichment; the Y-axis indicates the percentage of genes or −log10 (*p*-value); the Yellow line indicates log10 (*p*-value).

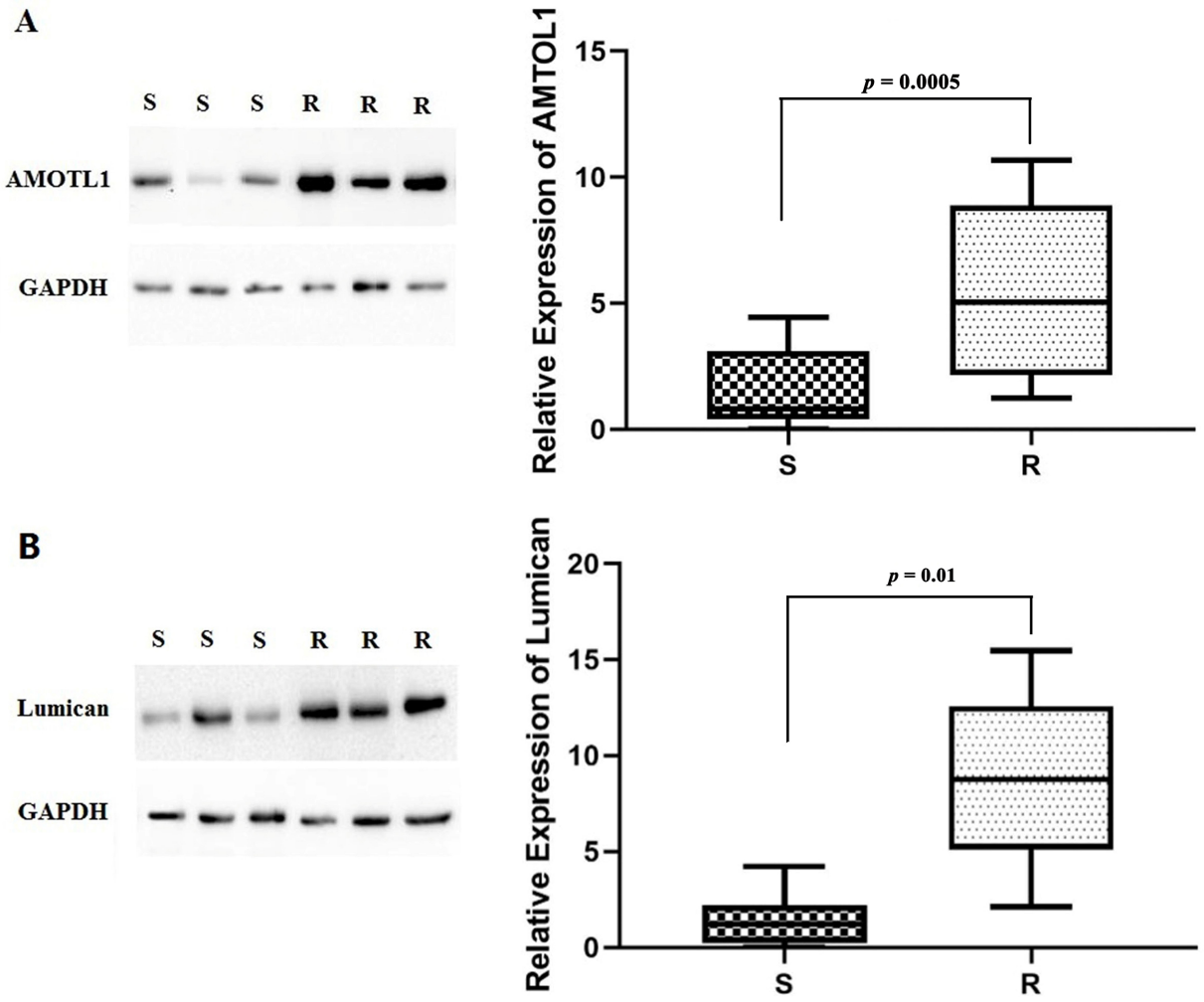

FIGURE 2. Western blotting of isobaric tags. (A) Platinum-resistant samples showed significant up-regulation of the AMOTL1 protein compared to platinum-sensitive samples (p = 0.0005). (B) Protein expression of Lumican was significantly upregulated in platinum-resistant tumor samples compared to platinum-sensitive tumor samples (p = 0.01). Abbreviations: AMOTL1, Angiomotin-like protein 1; R, resistant; S, sensitive; GAPDH: glyceraldehyde-3-phosphate dehydrogenase.

pressed proteins in platinum-resistant samples compared to platinum-sensitive samples, including 416 downregulated and 325 upregulated proteins. Among the upregulated proteins in EOC, two might be potentially related to platinum resistance (AMOTL1 and Lumican). We validated the expression of AMOTL1 and Lumican in ovarian cancer samples with varying chemosensitivities (sensitive and resistant) using Western blotting. In the EOC samples with platinum resistance, the two proteins were upregulated in agreement with the iTRAQ analysis results.

AMOTL1 (NCBI Accession Code NM_130847) is part of the angiomotin (Amot) proteins family and has been reported to exert important functions during tumorigenesis through the regulation of cellular migration, tube formation, and angiogenesis [13]. The Amot family comprises AMOT (p80 and p130 isoforms), AMOTL1, and AMOTL2 [14]. AMOTL1 is a 956 amino acid protein with a predicted molecular mass of about 106 kDa. In addition to its well-characterized functions, AMOTL1 plays a crucial role in apical-basal polarity and cytoskeleton stability. Different types of cell junction complexes were found to be involved in apical-basal polarity, including adherens junctions, gap junctions, desmosomes, basal lamina hemidesmosomes and apical tight junctions [15, 16]. According to the results from a large cohort of human breast cancers, AMOTL1 levels were upregulated throughout the course of cancer progression, and AMOTL1 expression in lymph node metastases was associated with a high risk of recurrence [17]. The Hippo signaling pathway is critical for many cellular behaviors, such as proliferation, survival, and cell contact inhibition [18]. Several studies showed that AMOTL1 is an important regulator of the Hippo pathway, playing a significant role in regulating the subcellular localization of the co-activators YAP (Yes-associated protein) and TAZ (transcriptional co-activator with PDZ-binding motif) [19, 20]. Our present study showed that AMOTL1 expression was increased in platinum-resistant EOC samples, which might contribute to tumor metastasis and chemotherapy resistance. The upregulation of AMOTL1 in platinum-resistant EOC samples may contribute to tumor metastasis and chemotherapy resistance, and further study of the association between AMOTL1 and the Hippo pathway may enhance our understanding of the mechanisms underlying chemoresistant EOC.

Lumican is a member of the small leucine-rich proteoglycan (SLRP) family, a type of proteoglycan found in the extracellular matrix (ECM) [21]. The expression of ECM components, such as proteoglycans and collagens, in cancer cells and stroma, has been closely related to tumor resistance to chemotherapy [22]. These ECM components influence cancer cells and elicit their resistance through the inhibition of apoptosis [23]. The small leucine-rich proteoglycan, Lumican, was found to be significant in maintaining the integrity of ECM [24]. In addition to its functions in regulating extracellular water and collagen fiber formation, Lumican also regulates tumor growth, adhesion, and migration [25, 26]. Despite contradictory findings regarding the effects of Lumican on cancer, its involvement in tumor growth, cell motility, and ECM attachment has been clearly demonstrated [27]. Seya *et al.* [28] reported that Lumican expression was correlated with tumor invasion, lymph node metastasis, and a significantly lower survival rate in patients with advanced colorectal cancer. Additionally, an increased expression of Lumican mRNA and protein was found in ovarian cancer cell lines resistant to drugs. Lumican expression in cytostatic-resistant cell lines may be critical for drug resistance [29]. In this present study, Lumican was shown to be upregulated in platinum-resistant EOC samples, which could be a contributing factor to cancer metastasis and resistance to chemotherapeutics.

6. Conclusions

Through proteomic analysis, we identified changes in the expression level of proteins of platinum-resistant and platinum-sensitive HGSC samples. The iTRAQ analysis identified AMOTL1 and Lumican as potential targets for modulating tumor growth, metastasis, resistance to chemotherapy, and recurrence. Furthermore, Western blotting was conducted to validate the expression of MOTL1 and Lumican at protein levels in platinum-resistant HGSC. Despite the interesting findings reported, there were several limitations worth considering. First, it should be noted that since this study had a relatively small number of participants, the results might be limited in providing pilot information on whether platinum resistance can be predicted in ovarian cancer. Second, the current study was conducted in a single center, and sample size limitations precluded western blotting validation on a completely independent cohort. Therefore, our findings may not be generalizable to other populations. Third, there are no commercially available assays for the biomarkers identified in this study, limiting their clinical application.

In summary, our study sheds light on the mechanisms underlying chemotherapy resistance and identifies AMOTL1 and Lumican as potential targets for clinical trials. However, further validation in a larger clinical cohort is necessary to determine their prognostic significance in HGSC.

AVAILABILITY OF DATA AND MATERIALS

The data presented in this study are available on reasonable request from the corresponding author.

AUTHOR CONTRIBUTIONS

YWu—designed the research study. YWa—conducted the research, performed data analysis, and drafted the paper.

ETHICS APPROVAL AND CONSENT TO PARTICIPATE

The protocol approval was granted by the Ethics Committee of the Beijing Shijitan Hospital, Capital Medical University (Ethical approval number: IEC-B-03-V01-FJ1). Before surgery, all cases and their families signed written informed consent forms. The World Medical Association's Code of Ethics (Declaration of Helsinki, 1964; revised in 2004) governed all procedures.

ACKNOWLEDGMENT

We are sincerely grateful towards Hongxia Li for her exceptional assistance in laboratory.

FUNDING

The present study was supported by the Beijing Obstetrics and Gynecology Hospital, Capital Medical University (FCYY202014).

CONFLICT OF INTEREST

The authors declare no conflict of interest.

REFERENCES

[1] Wang X, Xu X, Jiang G, Zhang C, Liu L, Kang J, *et al*. Dihydrotanshinone I inhibits ovarian cancer cell proliferation and migration by transcriptional repression of PIK3CA gene. Journal of Cellular and Molecular Medicine. 2020; 24: 11177–11187.

[2] Armstrong DK, Alvarez RD, Bakkum-Gamez JN, Barroilhet L, Behbakht K, Berchuck A, *et al*. Ovarian cancer, version 2.2020, NCCN clinical practice guidelines in oncology. Journal of the National Comprehensive Cancer Network. 2021; 19: 191–226.

[3] Coleridge SL, Bryant A, Kehoe S, Morrison J. Chemotherapy versus surgery for initial treatment in advanced ovarian epithelial cancer. Cochrane Database of Systematic Reviews. 2021; 2: CD005343.

[4] van Zyl B, Tang D, Bowden NA. Biomarkers of platinum resistance in ovarian cancer: what can we use to improve treatment. Endocrine-Related Cancer. 2018; 25: R303–R318.

[5] Lee H, Kwon OB, Lee JE, Jeon YH, Lee DS, Min SH, *et al*. Repositioning trimebutine maleate as a cancer treatment targeting ovarian cancer stem cells. Cells. 2021; 10: 918.

[6] Zhu M, Wang J, Wuna Y, Wang Y, Li H. Research progress in the treatment of partial platinum-sensitive recurrent ovarian cancer. Zhong Nan Da Xue Xue Bao Yi Xue Ban. 2021; 46: 644–652.

[7] Vianello C, Cocetta V, Catanzaro D, Dorn GW, De Milito A, Rizzolio F, *et al*. Cisplatin resistance can be curtailed by blunting Bnip3-mediated mitochondrial autophagy. Cell Death & Disease. 2022; 13: 398.

[8] Dettmer K, Stevens AP, Fagerer SR, Kaspar H, Oefner PJ. Amino acid analysis in physiological samples by GC-MS with propyl chloroformate derivatization and iTRAQ-LC-MS/MS. Methods in Molecular Biology. 2019; 393: 173–190.

[9] Li Y, Guo T, Wang X, Ni W, Hu R, Cui Y, *et al*. ITRAQ-based quantitative proteomics reveals the proteome profiles of MDBK cells infected with bovine viral diarrhea virus. Virology Journal. 2021; 18: 119.

[10] Swiatly A, Horala A, Matysiak J, Hajduk J, Nowak-Markwitz E, Kokot ZJ. Understanding ovarian cancer: iTRAQ-based poteomics for biomarker discovery. International Journal of Molecular Sciences. 2018; 19: 2240.

[11] Xu S, Wang Y, Li Y, Zhang L, Wang C, Wu X. Comprehensive analysis of inhibitor of differentiation/DNA-binding gene family in lung cancer using bioinformatics methods. Bioscience Reports. 2020; 40: BSR20193075.

[12] Vescarelli E, Gerini G, Megiorni F, Anastasiadou E, Pontecorvi P, Solito L, *et al*. MiR-200c sensitizes olaparib-resistant ovarian cancer cells by targeting Neuropilin 1. Journal of Experimental & Clinical Cancer Research. 2020; 39: 3.

[13] Zhou Y, Zhang J, Li H, Huang T, Wong CC, Wu F, *et al*. AMOTL1 enhances YAP1 stability and promotes YAP1-driven gastric oncogenesis. Oncogene. 2020; 39: 4375–4389.

[14] Lv M, Shen Y, Yang J, Li S, Wang B, Chen Z, *et al*. Angiomotin family members: oncogenes or tumor suppressors? International Journal of Biological Sciences. 2017; 13: 772–781.

[15] Drubin DG, Nelson WJ. Origins of cell polarity. Cell. 1996; 84: 335–344.

[16] Miyoshi J, Takai Y. Structural and functional associations of apical junctions with cytoskeleton. Biochim Biophys Acta. 2008; 1778: 670–691.

[17] Couderc C, Boin A, Fuhrmann L, Vincent-Salomon A, Mandati V, Kieffer Y, *et al*. AMOTL1 promotes breast cancer progression and is antagonized by Merlin. Neoplasia. 2016; 18: 10–24.

[18] Delgado ILS, Carmona B, Nolasco S, Santos D, Leitão A, Soares H. MOB: pivotal conserved proteins in cytokinesis, cell architecture and tissue homeostasis. Biology. 2020; 9: E413.

[19] Chan SW, Lim CJ, Chong YF, Pobbati AV, Huang C, Hong W. Hippo pathway-independent restriction of TAZ and YAP by angiomotin. Journal of Biological Chemistry. 2011; 286: 7018–7026.

[20] Oka T, Schmitt AP, Sudol M. Opposing roles of angiomotin-like-1 and zona occludens-2 on pro-apoptotic function of YAP. Oncogene. 2012; 31: 128–134.

[21] Chen X, Li X, Hu X, Jiang F, Shen Y, Xu R, *et al*. LUM expression and its prognostic significance in gastric cancer. Frontiers in Oncology. 2020; 10: 605.

[22] Di Paolo A, Bocci G. Drug distribution in tumors: mechanisms, role in drug resistance, and methods for modification. Current Oncology Reports. 2007; 9: 109–114.

[23] Croix BS, Kerbel RS. Cell adhesion and drug resistance in cancer. Current Opinion in Oncology. 1997; 9: 549–556.

[24] Brézillon S, Untereiner V, Mohamed HT, Ahallal E, Proult I, Nizet P, *et al*. Label-free infrared spectral histology of skin tissue part II: impact of a lumican-derived peptide on melanoma growth. Frontiers in Cell and Developmental Biology. 2020; 8: 377.

[25] Moseley R, Stewart JE, Stephens P, Waddington RJ, Thomas DW. Extracellular matrix metabolites as potential biomarkers of disease activity in wound fluid: lessons learned from other inflammatory diseases? British Journal of Dermatology. 2004; 150: 401–413.

[26] Neill T, Schaefer L, Iozzo RV. Decoding the matrix: instructive roles of proteoglycan receptors. Biochemistry. 2015; 54: 4583–4598.

[27] Hsiao KC, Chu PY, Chang GC, Liu KJ. Elevated expression of lumican in lung cancer cells promotes bone metastasis through an autocrine regulatory mechanism. Cancers. 2020; 12: 233.

[28] Seya T, Tanaka N, Shinji S, Yokoi K, Koizumi M, Teranishi N, *et al*. Lumican expression in advanced colorectal cancer with nodal metastasis correlates with poor prognosis. Oncology Reports. 2006; 16: 1225–1230.

[29] Klejewski A, Sterzyńska K, Wojtowicz K, Świerczewska M, Partyka M, Brązert M, *et al*. The significance of lumican expression in ovarian cancer drug-resistant cell lines. Oncotarget. 2017; 8: 74466–74478.

How to cite this article: Yuanjing Wang, Yumei Wu. iTRAQ-based proteomics analysis reveals novel candidates for platinum resistance of epithelial ovarian cancer. European Journal of Gynaecological Oncology. 2023; 44(5): 11-20. doi: 10.22514/ejgo.2023.074.